

# Solvent Mediated Superexchange in a C-Clamp Shaped Donor-Bridge-Acceptor Molecule: The Correlation between Solvent Electron Affinity and Electronic Coupling

Andrew M. Napper,<sup>†,§</sup> Ian Read,<sup>†</sup> Ruth Kaplan,<sup>‡</sup> Matthew B. Zimmt,<sup>\*,‡,||</sup> and David H. Waldeck<sup>\*,†,⊥</sup>

Department of Chemistry, University of Pittsburgh, Pittsburgh, Pennsylvania 15260, Department of Chemistry, Brown University, Providence, Rhode Island 02912, and Department of Math and Science, Chadron State College, Chadron, Nebraska 69337

Received: December 13, 2001; In Final Form: February 20, 2002

The temperature dependence of intramolecular electron-transfer rate constants for a C-shaped donor-bridge-acceptor molecule was measured in a series of solvents of differing electron affinities. The rate data was analyzed using a semiclassical version of the Marcus equation. The reaction free energies were characterized using a molecular model for solvation. The electronic coupling between the electron donor and acceptor groups is enhanced in solvents with more positive electron affinity. This enhancement arises from solvent occupation of a cleft between the donor and acceptor groups, resulting in an increase of the electronic coupling via an enhancement of the superexchange interaction. Solvents with more positive electron affinity provide mediating, superexchange states whose energies are closer to that of the resonant, initial, and final states.

## Introduction

Electron-transfer reactions remain of fundamental and practical importance. The understanding of how energetic factors, such as reorganization energy and reaction free energy, impact reaction rates is well established; however, our ability to model or calculate these properties remains limited.<sup>1,2</sup> For electron-transfer reactions in the nonadiabatic limit, the transfer process is well described by an electron tunneling mechanism. In this scenario, rearrangement of the surrounding medium, consisting of both intramolecular (innersphere) and intermolecular (outersphere) nuclear motions, allows exploration of those parts of phase space where the initial and final electronic states are in resonance. Electron transfer occurs in this crossing region, although the system may pass through it many times before the transfer event.<sup>3</sup> The electronic coupling matrix element  $|V|$  is a measure of the interaction energy between the initial and final electronic states in the crossing region and is directly related to the electron-transfer rate constant.<sup>4</sup> This study explores how the electronic coupling, or electron tunneling, between an electron donor and electron acceptor depends on the electronic structure of an intervening molecule. A correlation between the electronic coupling and the electron affinity of the intervening molecule is identified.

This study uses molecule **1** which contains an electron donor (D) and electron acceptor (A) that are joined together by a “rigid” saturated bridge (a DBA molecule).<sup>5</sup> Chart 1 provides a space filling, CPK rendering of **1** that illustrates the vacant “cleft” which lies directly between the donor and acceptor groups. For a molecule of this topology, electron tunneling through the cleft occurs in addition to tunneling mediated by

the covalent linkages of the bridge. Previous work<sup>2,6</sup> has shown that the presence of a solvent molecule within the cleft enhances the rate of tunneling as compared to that through the bridge. The simultaneous interaction of the solvent, e.g., 1,2,4-trimethylbenzene (Chart 1), with the donor and acceptor groups is believed to cause the enhancement. An earlier study found that increasing the size of alkyl substituents on aromatic solvents reduces the electronic coupling magnitude because bulky alkyl groups, such as isopropyl, impede access of the solvents’ aromatic core to the cleft of **1**. In contrast, the current work explores how the electronic coupling depends on the *electronic* characteristics of the substituted benzene, rather than on its steric bulk.

In the nonadiabatic limit, Fermi’s Golden Rule can be used to calculate the electron-transfer rate constant,  $k_{\text{et}}$

$$k_{\text{et}} = \frac{2\pi}{\hbar} |V|^2 \text{FCWDS} \quad (1)$$

$|V|$  is the donor/acceptor electronic coupling, and FCWDS is the Franck–Condon weighted density of states, which accounts for the nuclear rearrangement that must precede the electron tunneling event. Among solvents that provide similar FCWDS factors, the donor–acceptor electronic coupling will determine the relative magnitudes of the transfer rate constants. Molecules that lie between the donor and acceptor can enhance the electronic coupling through interaction of their molecular orbitals with those of the donor and acceptor. When the electronic coupling is weak enough, it can be calculated using a perturbation theory approach, known as superexchange.<sup>7</sup> The superexchange mechanism predicts a dependence of the electronic coupling on the energy of electronic states that mediate the electron’s (or a hole’s) movement from donor to acceptor. Previous studies have suggested that electron mediated superexchange is more important than hole mediated superexchange for the transfer of an electron from the locally excited state of **1**.<sup>8</sup> For a single site between the donor and acceptor (see Figure

\* To whom correspondence should be addressed.

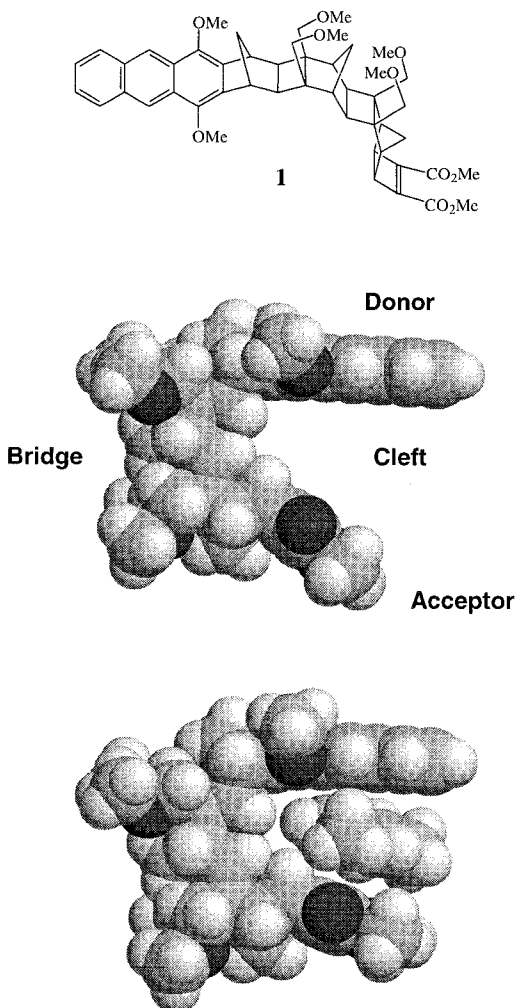
<sup>†</sup> Department of Chemistry, University of Pittsburgh.

<sup>‡</sup> Department of Chemistry, Brown University.

<sup>§</sup> Department of Math and Science, Chadron State College.

<sup>||</sup> E-mail: Matthew\_Zimmt@brown.edu.

<sup>⊥</sup> E-mail: dave@pitt.edu.

**CHART 1: Line Structure and Space-filling Representations of 1<sup>a</sup>**


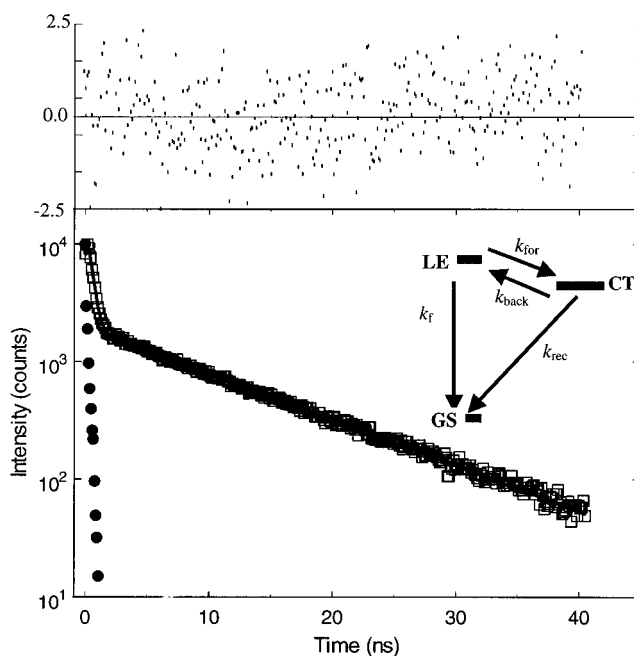
<sup>a</sup> In the bottom part, a space-filling model with 1,2,4-trimethylbenzene in the cleft of **1** is shown.

2), the superexchange expression for an electron-mediated process is given by

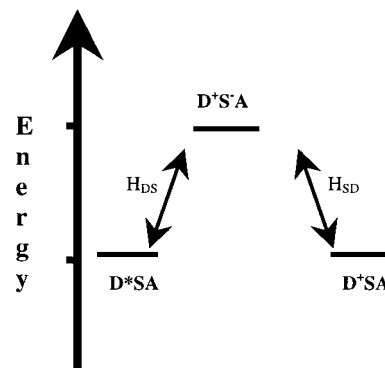
$$|V| = \frac{H_{D^*S}H_{SA}}{E_{D^*S-A} - E_{D^*SA}} \quad (2)$$

where  $H_{D^*S}$  and  $H_{SA}$  are the donor/solvent and solvent/acceptor exchange integrals, respectively.  $E_{D^*SA}$  and  $E_{D^*S-A}$  represent the energies of the transition state and the vertically displaced superexchange state ( $D^+S^-A$ ). By using solvents with differing vertical electron affinities ( $EA_v$ ), it should be possible to manipulate the size of the denominator in eq 2 and tune  $|V|$ . In particular, solvents that are more favorable toward electron attachment (more positive values of  $EA_v$ ) are predicted to stabilize the superexchange state  $D^+S^-A$  and enhance the total electronic coupling,  $|V|$ .

Previous studies of solvent mediated superexchange with **1** identified a significantly larger value of the electronic coupling for benzonitrile in the cleft than for benzene or alkylbenzenes. The current study explores how the solvent molecule's electronic character affects the size of the superexchange coupling. The earlier data in benzonitrile and alkylbenzene solvents showed that methyl substitution of the aromatic ring reduced the electronic coupling slightly. By contrast, those studies showed that multiple isopropyl groups on a benzene kept its aromatic



**Figure 1.** A fluorescence decay profile is shown for **1** in 2,5-dichlorotoluene at 338 K. The best fit parameters are 311 ps (90%), 11.15 ns (10%) and a  $\chi^2$  of 1.14. The top graph plots the residuals for the best-fit decay law (thick line through data points). For clarity, only every tenth data point is plotted here. The inset shows the level kinetics used to interpret these data.



**Figure 2.** This diagram illustrates the energy level scheme that is used in the superexchange model to calculate  $|V|$ .

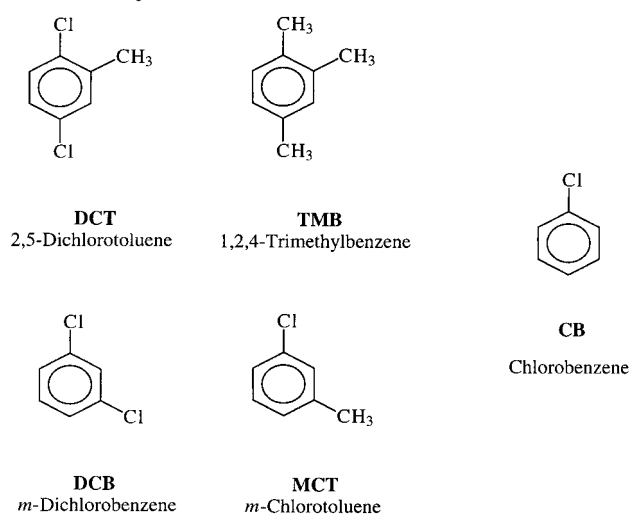
core out of the cleft of **1**. The current study compares the coupling provided by methyl-substituted aromatic solvents with correspondingly substituted chloro aromatic solvents (see Chart 2). The similar size of methyl and chloro groups should produce similar steric effects, thus allowing the electronic effects to be identified (the new feature of this study). Two pairs of solvents (pair 1: *meta*-chlorotoluene/*meta*-dichlorobenzene; pair 2: 2,5-dichlorotoluene/1,2,4-trimethylbenzene) are investigated. The solvents in each pair have significantly different electron affinity, but have similar sizes, shapes, and electrostatic properties (see Table 2) and should give rise to similar FCWDS terms. The *meta*-chlorotoluene/*meta*-dichlorobenzene pair was chosen because it is moderately polar, and the 2,5-dichlorotoluene/1,2,4-trimethylbenzene pair was chosen because it is weakly polar and should allow an accurate determination of the reaction free energies. To the extent that the FCWDS factors are the same for each solvent pair, a direct comparison of the electron transfer rate constants can be ascribed directly to variation of the coupling magnitude,<sup>9</sup> and the correlation between  $|V|$  and solvent electron affinity may then be analyzed.

**TABLE 1: Reaction Free Energies  $\Delta_r G$ , Reorganization Energies  $\lambda_o$ , and FCWDS Are Given at  $T = 295$  K for the Electron Transfer Reaction Using Different Models<sup>a</sup>**

solvent <sup>c</sup>	continuum <sup>b</sup>			molecular			from $k(T)$ data	
	$\Delta_r G$ , eV	$\lambda_o$ , eV	FCWDS, eV <sup>-1</sup>	$\Delta_r G$ , eV	$\lambda_o$ , eV	FCWDS, eV <sup>-1</sup>	$\Delta_r G$ , eV	$\lambda_o$ , eV
mesitylene	-0.19	0.0038	50	-0.044	0.06	6.7	-0.039	0.03
toluene	-0.20	0.016	30	-0.090	0.09	6.8	-0.089	0.09
benzene	-0.19	0.0045	47	-0.11	0.10	6.3	-0.11	0.10
TMB	-0.20	0.013	31	-0.054	0.07	3.7	-0.057	0.09
DCT	-0.26	0.053	15	-0.10	0.15	0.053	-0.10	0.15
DCB	-0.35	0.14	13	-0.28	0.32	0.25		0.60 ± 0.08
MCT	-0.35	0.14	13	-0.31	0.36	2.8		0.39 ± 0.03
CB	-0.32	0.14	13	-0.32	0.33	1.5		0.47 ± 0.04
benzonitrile	-0.47	0.28	12	-0.52	0.52	0.084		1.06 ± 0.05

<sup>a</sup> The error estimates in the polar solvents represent the effect of different models for the reaction free energy's temperature dependence. See text for details. <sup>b</sup> The solute parameters used in both calculations are 8.51 Å for the cavity radius, 34 D for the CT state dipole moment, and 0.08 eV for the gas-phase driving force. Relevant solvent parameters are reported in Table 2. <sup>c</sup> Solvent abbreviations correspond to the structures in Chart 2.

### CHART 2: Molecular Structures for the Five Solvents in This Study<sup>a</sup>



<sup>a</sup> Their abbreviations are included for easy reference.

This work proceeds by measuring the electron-transfer rates as a function of temperature in each of the solvents. Extracting the electronic coupling from the data requires an accurate modeling of the FCWDS in each solvent as a function of temperature. Use of different FCWDS models yields different estimates of the coupling, but *relative* coupling magnitudes in different solvents are robust to changes in the FCWDS model [these affects have been discussed elsewhere<sup>10</sup>]. The results are analyzed using two different models for the FCWDS: a dielectric continuum treatment and a molecular based treatment. The molecular treatment is the same as that used previously to describe the temperature-dependent electron-transfer rate constant and reaction free energy in a series of alkyl-substituted benzenes.<sup>6</sup> This study extends the application of this model to the more polar chlorobenzene solvents and benzonitrile, identifying its limitations for characterizing the reaction free energy, solvent reorganization energy and their temperature dependencies. A dielectric continuum treatment is also used to model the FCWDS. This model is expected to provide reasonable estimates in the polar solvents and act as a point of reference for the molecular treatment. Combining these models for  $\Delta_r G$  with previous results for the internal reorganization energy parameters, allows the solvent dependent reorganization energy  $\lambda_o(T)$  and the electronic coupling magnitude  $|V|$  to be determined from the temperature dependence of the rate constant. The correlation of  $|V|$  with the solvent's electronic character could then be analyzed.

### Background

The single-mode semiclassical expression for the FCWDS models interactions with the solvent classically and treats solute vibrations using a single effective high-frequency, quantum mechanical, mode.<sup>1b,11</sup> The rate constant expression is

$$k_{\text{et}} = \frac{4\pi^2}{h} |V|^2 \frac{1}{\sqrt{4\lambda_o \pi k_B T}} \sum_{n=0}^{\infty} \exp(-S) \left( \frac{S^n}{n!} \right) \times \exp \left[ -\frac{(\Delta_r G + \lambda_o + nh\nu)^2}{4\lambda_o k_B T} \right] \quad (3)$$

This equation has five parameters:  $\Delta_r G$  (the change in reaction Gibbs free energy),  $\lambda_o$  (low frequency—primarily solvent—reorganization energy),  $\lambda_i$  (high frequency—primarily solute—reorganization energy),  $\nu$  (the effective frequency of the quantum mechanical mode), and  $|V|$  (donor/acceptor electronic coupling).  $S$  (the Huang—Rhys factor) is defined as

$$S = \frac{\lambda_i}{h\nu} \quad (4)$$

Of these five parameters,  $\lambda_i$  and  $\nu$  can be estimated from analysis of charge-transfer absorption and emission spectra.<sup>10,11</sup> Typically,  $\Delta_r G$  and  $\lambda_o$  are estimated using a theoretical model. In this study,  $\Delta_r G$  was determined experimentally in the weakly dipolar solvents, where its magnitude was within 0.1 eV of zero, and was modeled in the more polar solvents of the series. The molecular model employed (vide infra) provides  $\Delta_r G$  values that are in reasonable agreement with the experimental values from the weakly polar solvents and with predictions of a dielectric continuum model for the highly polar solvents. Once reliable values of  $\Delta_r G$ ,  $\lambda_i$ , and  $\nu$  have been obtained, the electronic coupling matrix element  $|V|$  and the solvent reorganization energy  $\lambda_o(T)$  can be extracted from analysis of the temperature-dependent rate constant by way of eq 3.

**Continuum Approaches to  $\Delta_r G$  and  $\lambda_o$ .** The simplest means of estimating  $\Delta_r G$  and  $\lambda_o$  is to use a dielectric continuum model for the solute—solvent interaction. Such treatments have been used successfully to describe the solvent reorganization energy and reaction free energy for electron transfer in polar solvents. The continuum model used here treats the charge-separated state as a point dipole  $\mu$  embedded in a spherical cavity that is immersed in a dielectric continuum. This description of the solute shape and electrostatic character is the same as that used in the molecular model and allows a direct comparison between

the two treatments. The continuum reorganization energy  $\lambda_o$  is given by

$$\lambda_{o,\text{cont}} = \frac{\mu^2}{a_0^3} \left( \frac{\epsilon - 1}{2\epsilon + 1} - \frac{n^2 - 1}{2n^2 + 1} \right) \quad (5)$$

where  $a_0$  is the effective cavity radius,  $\epsilon$  is the static dielectric constant of the solvent, and  $n$  is the refractive index of the solvent. In this same approximation the reaction Gibbs free energy can be written as

$$\Delta_r G = \Delta_{\text{vac}} G - \left[ \frac{\mu^2}{a_0^3} \right] \left( \frac{\epsilon - 1}{2\epsilon + 1} \right) \quad (6)$$

where  $\Delta_{\text{vac}} G$  is the reaction Gibbs free energy in the absence of solvation. Although this continuum treatment of the solute–solvent interaction is useful in some situations, recent results<sup>2</sup> have shown that a molecular approach provides more accurate values of  $\Delta_r G$  and  $\lambda_o$  for weakly dipolar solvents and especially for aromatic solvents where quadrupole interactions are important. A number of workers have constructed more elaborate models for the solvent cavity<sup>10,12</sup> and the medium's dielectric response.<sup>13</sup> As a point of reference, the spherical cavity dielectric continuum model is used to predict values for  $\lambda_o$  (outersphere reorganization energy),  $\Delta_r G$ , and the FCWDS for the solvents studied here, see Table 1.

**Molecular Approach to  $\Delta_r G$  and  $\lambda_o$ .** Previous work showed<sup>6</sup> that a molecular description of solute–solvent interactions was important for accurately characterizing the reorganization energy, the reaction free energy, and their temperature dependencies in aromatic solvents. Matyushov<sup>14</sup> has developed a model that treats the solute and solvent molecules as polarizable spheres, with imbedded point dipole moments, and, in the case of solvent, an imbedded point quadrupole moment. The solute dipole moment magnitude  $\mu$  is given by  $\Delta q R_{\text{DA}}$ , in which  $\Delta q$  is the charge transferred from the donor to the acceptor and  $R_{\text{DA}}$  is the charge separation distance. This model was successfully used to simulate the solvent and temperature dependencies of the reaction free energy for **1** in a series of six alkylbenzene solvents using only four parameters to represent the solute.<sup>2</sup> The molecular model treats the reaction free energy as a sum of four components

$$\Delta_r G = \Delta_{\text{vac}} G + \Delta_{\text{dqi}} G^{(1)} + \Delta_{\text{disp}} G + \Delta_i G^{(2)} \quad (7)$$

in which  $\Delta_{\text{vac}} G$  corresponds to the reaction free energy in a vacuum and the other three terms account for solvation effects. This earlier study showed that the electrostatic and induction terms ( $\Delta_{\text{dqi}} G^{(1)}$  and  $\Delta_i G^{(2)}$ ) make the dominant contributions to the solvation free energy and that the dispersion term  $\Delta_{\text{disp}} G$  plays a minor part and may be ignored. The reorganization energy was expressed as a sum of three terms

$$\lambda_o = \lambda_p + \lambda_{\text{ind}} + \lambda_{\text{disp}} \quad (8)$$

in which  $\lambda_p$  accounts for solvent reorganization arising from electrostatic interactions,  $\lambda_{\text{ind}}$  is the contribution from induction forces, and  $\lambda_{\text{disp}}$  accounts for dispersion interactions. A more detailed description of this model and its application to **1** may be found elsewhere.<sup>2</sup>

**Internal Reorganization Parameters.** The internal reorganization energy  $\lambda_i$  and the effective frequency  $\nu$  significantly influence the quantitative data analysis, but do not have a significant solvent dependence. Although the absolute value of the electronic couplings that are extracted from the measured

electron-transfer rates depend on the values used for the internal reorganization parameters, the relative coupling magnitudes for **1** in different solvents do not depend on the values used for the internal reorganization parameters. The correlation between parameters in this system is discussed at length elsewhere.<sup>10</sup> The value used for  $\lambda_i$  is 0.39 eV and that used for  $\nu$  is 1412  $\text{cm}^{-1}$ . These are the same values that were used in previous studies<sup>2,6</sup> and were obtained through a combination of quantum chemical calculations and the analysis of charge-transfer spectra.

**Kinetic Analysis.** Photoexcitation of the anthracene donor moiety creates a locally excited state that is slightly higher in energy than the charge separated state. Figure 1 shows the level kinetics scheme that is used to describe the decay of the locally excited (LE) state prepared by the light pulse. In highly dipolar solvents where  $k_{\text{back}}$  is small, the fluorescence decay of the locally excited state is single exponential with a decay constant that is the sum of the forward electron-transfer rate constant  $k_{\text{for}}$  and the intrinsic fluorescence decay rate constant of the chromophore. By measuring the deactivation of the locally excited state ( $k_f$ ) in an analogue of **1** that has no electron acceptor, it is possible to extract the electron transfer rate constant. This procedure can be used to assess any contributions from the external heavy atom effect or exciplex formation with chlorinated aromatic solvents and quantitatively account for them. The fluorescence decay rate of the donor only compound does not change in any significant way with the chlorine content of the solvent (see the Supporting Information and ref 8). To reiterate, the analysis assumes that the difference in fluorescence decay between the locally excited state of **1** and a donor only control compound in the same solvent arises from the electron-transfer deactivation channel in **1**.

In weakly dipolar solvents the fluorescence decay law becomes double exponential because  $k_{\text{back}}$  is no longer small. In this case the analysis must account for the excited-state equilibrium and provides the three rate constants:  $k_{\text{for}}$ ,  $k_{\text{back}}$ , and  $k_{\text{rec}}$  [see footnote 15 for details of this analysis]. The Gibbs free energy of the forward reaction is obtained from the ratio of the forward and back rate constants via

$$\Delta_r G = -RT \ln(k_{\text{for}}/k_{\text{back}}) \quad (9)$$

It is empirically found that  $\Delta_r G$  values  $\geq -0.1$  eV can be reliably determined. More negative values have a small amplitude of the second decay component, which causes large uncertainty in the determination of  $k_{\text{back}}$  and of  $\Delta_r G$ .

## Experimental Section

Solutions of **1** were prepared with an optical density of ca. 0.05 at the laser excitation wavelength, 375 nm. The preparation of **1** was reported elsewhere.<sup>16</sup> Chlorobenzene (99.9+%, HPLC grade), *m*-chlorotoluene (98%), *m*-dichlorobenzene (98%), 1,2,4-trimethylbenzene (98%), and 2,5-dichlorotoluene (98%) were purchased from Aldrich. The chlorinated solvents were dried over  $\text{CaCl}_2$  for 2 days, filtered, and then fractionally distilled using a vigreux column. The purified fractions were used immediately in all the experiments. 1,2,4-trimethylbenzene was dried with anhydrous magnesium sulfate, filtered, and then refluxed over sodium for 2 days. The solution was then fractionally distilled using a vigreux column, and the purified fraction was immediately used to prepare the sample. Each solution was freeze–pump–thawed a minimum of three times. The samples were back-filled with Ar to reduce evaporation at the higher experimental temperatures.

Excitation of the sample was performed at 375 nm by the frequency-doubled cavity-dumped output of a Coherent CR-



599-01 dye laser using LDS750 (Exciton) dye, which was pumped by a modelocked Coherent Antares Nd:YAG. The dye laser pulse train had a repetition rate of ca. 300 kHz. Pulse energies were kept below 1 nJ, and the count rates were kept below 3 kHz. All fluorescence measurements were made at the magic angle. Other specifics of the apparatus have been reported elsewhere.<sup>17</sup> The temperature cell was fabricated out of aluminum and was controlled by a NESLAB RTE-110 chiller. Temperatures were measured using a Type-K thermocouple (Fisher-Scientific), accurate to within 0.1 °C.

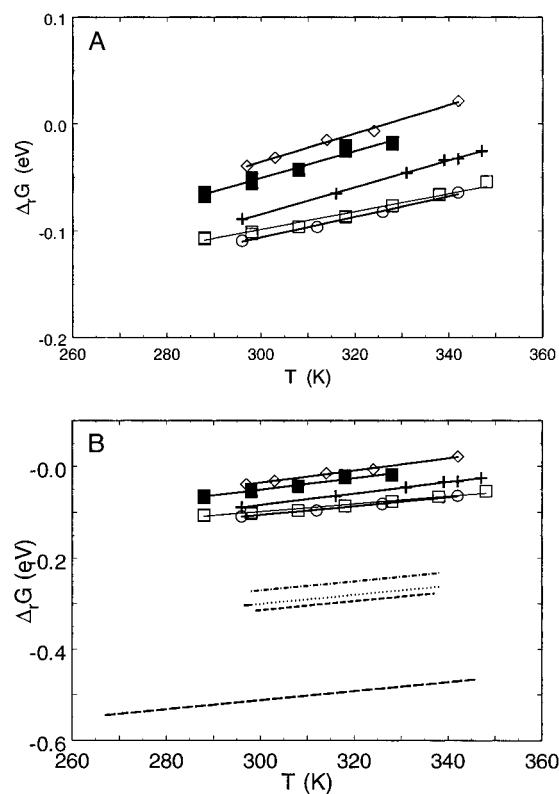
The fluorescence decays were fit to a sum of two exponentials using the Marquardt–Levenberg nonlinear least squares algorithm. Instrument response functions were measured using a sample of colloidal BaSO<sub>4</sub> in glycerol. Figure 1 shows a fluorescence decay from **1** in 2,5-dichlorotoluene at 338 K, the best fit to a sum of two-exponential and the fitting residuals.

Fitting to the semiclassical equation (eq 3) was performed using Microsoft Excel 2000. The FCWDS sum rapidly converges for the solvents in this study, and was not evaluated past the sixth term.

## Results and Discussion

Fluorescence decay profiles of **1** and its donor only analogue were measured in the five aromatic solvents shown in Chart 2. The rate data is provided in the Supplemental Information. The lifetimes obtained for the donor only compound in each solvent do not differ greatly and do not display a significant temperature dependence. The donor only compound's fluorescence lifetimes were not significantly different from lifetimes measured in previous studies,<sup>18</sup> muting possible concerns about the chlorinated aromatic solvents affecting the intrinsic photophysics of the dimethoxyanthracene moiety. The fluorescence decays from **1** in the different solvents were analyzed using the kinetic scheme in Figure 1. The decay profiles in 1,2,4-trimethylbenzene and 2,5-dichlorotoluene, the pair of solvents with the smallest dipole moments, had a significant long time constant component, which allowed an accurate determination of  $k_{\text{back}}$  and  $\Delta_r G$ . Although a second decay component could be identified in the more polar chlorinated solvents, a single exponential dominated the decay profiles, making it too difficult to reliably determine  $k_{\text{back}}$  and, hence,  $\Delta_r G$ . The amplitude of the long lifetime component correlated with the size of the solvent dipole moment, in accordance with its critical role in determining the solvation of the charge separated state. The present analysis is limited to the behavior of the forward rate constants, because they could be reliably determined for all of the solvents.

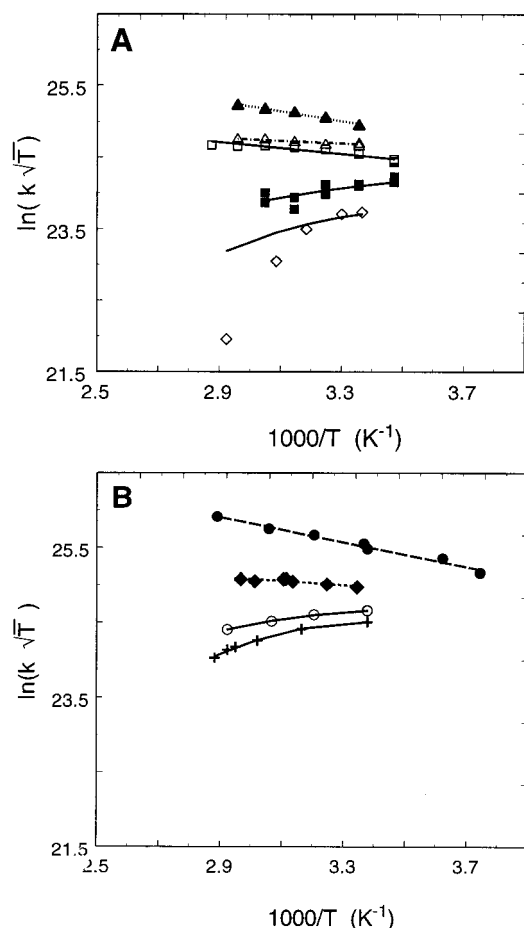
The charge separation rate constant for **1** in 2,5-dichlorotoluene is larger than that in 1,2,4-trimethylbenzene at all temperatures investigated (see Figure 4). The rate constant ratio varied from 1.5 at 295 K to 2.2 at 328 K. Determination of the relative electronic coupling magnitudes in these two solvents requires estimation of the FCWDS. Before proceeding with quantitative modeling of the reaction free energy  $\Delta_r G(T)$  and the outer sphere reorganization energy  $\lambda_o(T)$  by way of a molecular solvation model, it is useful to consider the predictions of a simple dielectric continuum model. The dielectric continuum treatment was used to predict the FCWDS terms at 295 K for each of the solvent pairs, 1,2,4-trimethylbenzene/2,5-dichlorotoluene and *m*-dichlorobenzene/*m*-chlorotoluene, see Table 1.<sup>19</sup> The continuum model estimate of the FCWDS factor in 2,5-dichlorotoluene is half of its value in 1,2,4-trimethylbenzene. Accordingly, the ratio of the square of the electronic coupling magnitudes is 3, via eq 3. This indicates that the electronic coupling for **1** in 2,5-dichlorotoluene is 75% larger



**Figure 3.** The experimental  $\Delta_r G$  data for 2,5-dichlorotoluene (open squares), 1,2,4-trimethylbenzene (filled squares), toluene (+), benzene (open circle), and mesitylene (open diamonds) are shown here. Panel A shows an expanded view of the data for which experimental  $\Delta_r G$  data are available. The best fit predictions from the molecular model are shown as solid lines for each data set (see text for details). Panel B shows the predicted free energies for all the solvents. The long dashed curve is the prediction for benzonitrile, the short dashed curve is the prediction for chlorobenzene, the dotted curve is the prediction for *m*-chlorotoluene, and the dashed–dotted curve is the prediction for *m*-dichlorobenzene.

than that in 1,2,4-trimethylbenzene. It is important to realize that the continuum model prediction for the FCWDS in this weakly polar pair of solvents may not be reliable; e.g., quadrupole contributions to the solvation could be quite different for the two solvents. For the *m*-dichlorobenzene/*m*-chlorotoluene pair, the charge separation rate constant of **1** in *m*-dichlorobenzene is larger than that of *m*-chlorotoluene at all temperatures (see Figure 4). At 295K the *m*-dichlorobenzene rate constant is 1.3 times larger. The continuum model predicts that the FCWDS for **1** in *m*-dichlorobenzene is the same as in *m*-chlorotoluene, so that the ratio of the squares of the electronic coupling terms is 1.3. This ratio gives an electronic coupling for **1** in *m*-dichlorobenzene that is about 15% larger than that in *m*-chlorotoluene. This analysis suggests that the difference in the electron transfer rate constants between the structurally similar solvents can be attributed, at least in part, to differences in the  $|V|$ . In addition, the continuum treatment provides a reference point for the molecular model described below.

**Molecular Model.** Quantitative modeling of the reaction free energy and the reorganization energy was performed with a molecular model that accounts for solvent dipole, polarizability and quadrupole interactions.<sup>2,14</sup> The solvent molecule parameters needed for the model are reported in Table 2. An earlier study demonstrated that this model accurately reproduces the magnitudes and temperature dependence of the reaction free energy in a homologous series of alkylbenzenes. The model has four parameters for the solute. For **1** in the alkylbenzene solvents,



**Figure 4.** The temperature-dependent rate data are fit to the semiclassical expression in each of the solvents. The data are plotted in two panels for clarity, however the axis scales are identical. Part A plots the data for *m*-dichlorobenzene (filled triangles), *m*-chlorotoluene (open squares), 2,5-dichlorotoluene (open squares), 1,2,4-trimethylbenzene (filled squares), and mesitylene (open diamonds). Part B plots the data for benzonitrile (filled circles), chlorobenzene (filled diamonds), benzene (open circles), and toluene (+). The lines represent best fit curves using the semiclassical equation (see Figure 3 for convention on line type).

these parameters were a cavity radius of 7.25 Å, a charge separated state dipole moment of 34 D, a solute molecular polarizability of 70 Å<sup>3</sup> and a vacuum reaction free energy,  $\Delta_{\text{vac}}G$ , of 0.34 eV.<sup>2</sup> Use of these parameters to calculate  $\Delta_rG$  in 2,5-dichlorotoluene generates a value that is 0.15 eV too exoergic. One can adjust the four solute parameters in an effort to improve the agreement between the experimental and calculated  $\Delta_rG$  values. However, it was not possible to produce an accurate fit of the free energy data in all the solvents as a function of temperature. It was possible to fit  $\Delta_rG$  at 295 K from 2,5-dichlorotoluene and from all of the alkylbenzene solvents. The parameters needed to accurately describe the data at 295 K were a cavity radius of 8.51 Å, a dipole moment of 34 D, a solute polarizability of 100 Å<sup>3</sup>, and a  $\Delta_{\text{vac}}G$  of 0.08 eV. The calculated solvent dependence of the free energy data is most sensitive to the cavity radius. The larger radius used for the fit at 295 K reduces the size of the electrostatic solvation and predicts a temperature dependence for the free energy that is much smaller than the experimentally observed dependence (e.g., the model predicts a free energy change for **1** in 2,5-dichlorotoluene of 0.025 eV from 295 to 347 K, whereas the observed change is 0.049 eV).

Figure 3 shows the reaction free energies for the solvents reported here as a function of temperature. It was found

empirically that the average temperature dependence of the reaction free energy in the alkylbenzene and dichlorotoluene solvents is about 1 meV/K. The solid lines in the figure show a linear fit to the reaction free energy's temperature dependence. The observed temperature dependencies are 0.83 meV/K for 2,5-dichlorotoluene, 1.1 meV/K for 1,2,4-trimethylbenzene, 0.96 meV/K for benzene, 1.2 meV/K for toluene, and 1.3 meV/K for mesitylene. The quality of the fit is evident in Figure 3A, which expands the free energy scale about the experimental values found in the weakly dipolar solvents. The average of these slopes is 1.1 meV/K. Because the reaction free energy is not available in the more polar solvents and a physical model is not available to guide the change in temperature dependence through the different solvent systems studied here, an empirical value of 1 meV/K was used in these solvents (vide infra).

Figure 3B shows the data of Figure 3A along with the reaction free energies that are predicted using the molecular solvation model and the new parameter set for **1** in chlorobenzene, *m*-chlorotoluene, *m*-dichlorobenzene, and benzonitrile.  $\Delta_rG$  in these solvents is too negative to be determined experimentally from the fluorescence decays. The molecular model predictions of the free energies at 295 K can be compared with the continuum model predictions (see Table 1). For the more polar solvents, i.e., for solvents with  $\epsilon_s \geq 5$ , the largest deviation between the two sets of predicted values occurs for *m*-dichlorobenzene and represents a 20% difference, 0.07 eV in magnitude. The continuum model and molecular model predictions deviate much more significantly in the nondipolar and weakly dipolar solvents, where the dielectric continuum treatment is expected to fail. The dielectric continuum model performs reasonably well for **1** in more polar solvents, as discussed previously for the electron transfer of **1** in acetonitrile and benzonitrile.<sup>10</sup> This agreement between the continuum model and the molecular model in the polar solvents and between the experimental measurements and the molecular model in the weakly dipolar solvents supports the reliability of the molecular model's  $\Delta_rG$  prediction at 295 K.

The electronic coupling magnitude can be determined from the rate data and eq 3 provided accurate values of the solvent reorganization energy and its temperature dependence are available. The failure of the molecular model, with the new parameter set, to reproduce the temperature dependence of  $\Delta_rG$  in this set of solvents requires use of an alternate method (vide infra) to evaluate  $\lambda_s$  and its temperature dependence. The results of the analysis are sensitive to the value used for the temperature derivative of  $\Delta_rG$ . To estimate the uncertainty in the derived values of the reorganization energy and the electronic coupling, three different values of  $d(\Delta_rG)/dT$  were used for solvents in which this quantity was not directly measured; benzonitrile, 1,3-dichlorobenzene, chlorobenzene, and 3-chlorotoluene. Because the temperature dependencies of the reaction free energy in the nonpolar and weakly polar solvents are clustered near 1 meV/K, this value was used as the best estimate. This is the value used for preparation of the plots shown in Figures 3 through 6. To estimate the error in this value for the reaction free energy's temperature dependence, an upper bound was obtained by using a slope of 2 meV/K and a lower bound was obtained by using the predicted slope from the continuum model.<sup>20</sup> Independent fits to the data were performed with these estimates and used to determine the upper and lower bounds on the solvent reorganization energy and the electronic coupling (see Tables 1 and 3).<sup>21</sup>

Given the difficulty in using the molecular model to quantitatively reproduce the temperature dependence of the

**TABLE 2: This Data Provides Physical Parameters of the Solvents Used in This Study**

solvent	$n_D^a$	$\epsilon^a$	IP, eV <sup>b</sup>	EA <sub>v</sub> , eV <sup>c</sup>	$\mu$ , D <sup>d</sup>	$\langle Q \rangle$ , D Å <sup>d</sup>	$\alpha$ , Å <sup>3e</sup>	$\sigma$ , Å	$\epsilon_{LJ}$ , K	$\eta$
mesitylene	1.50	2.27	8.4	-1.03	0.07	7.4	17.0	6.26	870	0.556
toluene	1.49	2.38	8.8	-1.11	0.29	7.8	12.4	5.66	704	0.538
benzene	1.50	2.28	9.2	-1.12	0.00	8.2	10	5.27	614	0.518
TMB	1.50	2.38	8.4–8.6	-1.07	0.30	7.3	17.0	6.26	865	0.562
DCT	1.55	3.01	8.8	-0.31	0.57	14	17.0	6.36	972	0.630
DCB	1.55	5.02	9.1	-0.31	2.03	10	13.2	5.97	882	0.587
MCT	1.52	5.55	8.7	-0.75	2.34	7.8	13.2	6.01	838	0.579
CB	1.52	5.62	9.1	-0.75	2.15	8.4	11.5	5.62	748	0.552
benzonitrile	1.53	25.9	9.7	0.24	4.85	15.2	12.5	5.69	741	0.565

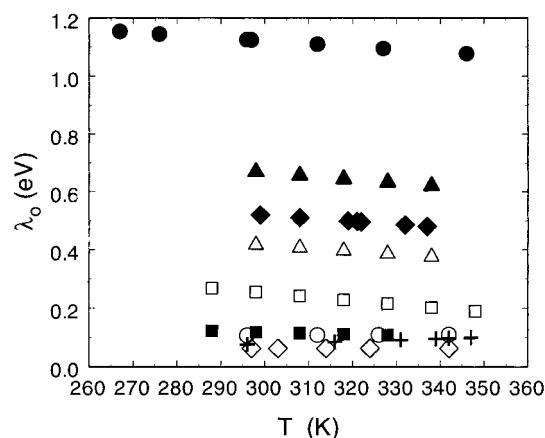
<sup>a</sup> See Chart 2 for solvent abbreviations. <sup>a</sup> Data were obtained from Landolt-Bornstein. The value for DCT was estimated using the Debye formula and the vacuum dipole moment. <sup>b</sup> NIST Webbook at [webbook.nist.gov](http://webbook.nist.gov). <sup>c</sup> Electron Affinities were obtained from ref 28. <sup>d</sup> The dipole moment and quadrupole moments were calculated at the RHF/6-31G\*\*//RHF/6-31G\*\* level using Gaussian 98. <sup>e</sup> Polarizabilities were obtained from the literature (*CRC Handbook*, 78th ed.; CRC Press: Boca Raton, FL, 1998), but optimized, by <10%, for a best fit of the  $\Delta_r G(295\text{ K})$  data. <sup>f</sup> The hard sphere diameter  $\alpha$  and the Lennard-Jones energy parameter  $\epsilon$  were obtained from the literature.<sup>28</sup> <sup>g</sup> The reduced packing density,  $\eta = \pi\rho\sigma^3/6$ , was determined using literature values of the density (*CRC Handbook* (vide supra)).

**TABLE 3: The Best Fit  $|V|$ , the Electron Affinity EA, and the Ionization Potential IP**

solvent <sup>a</sup>	$ V $ , cm <sup>-1</sup>	IP, <sup>b</sup> eV	EA, <sup>c</sup> eV
mesitylene	2.8	8.4	-1.03
toluene	4.7	8.8	-1.11
benzene	5.3	9.2	-1.12
TMB	4.6	8.4–8.6	-1.07
DCT	9.6	8.8	-0.31
DCB	22 ± 8	9.1	-0.31
MCT	7.3 ± 1	8.7	-0.75
CB	11 ± 2	9.1	-0.75
benzonitrile	55 ± 13	9.7	0.24

<sup>a</sup> Solvent abbreviations correspond to the structures in Chart 2. <sup>b</sup> The ionization potentials are taken from the NIST Webbook at [webbook.nist.gov](http://webbook.nist.gov). <sup>c</sup> The electron affinities are taken from ref 27. The error estimates in the polar solvents represent the effect of different models for the reaction free energy's temperature dependence. See text for details.

reaction free energies, the model was not employed to make predictions of the solvent reorganization energies, for which no direct experimental data is available. Nonetheless, it was possible to evaluate the temperature-dependent reorganization energy and the electronic coupling from the rate data using Eqn 3 and the available information. The temperature-dependent reorganization energy was determined from the temperature dependence of the rate data through the slope of the plot in Figure 4. The derivative,  $(\partial \ln(k_{et}\sqrt{T})/\partial(1/T))$ , was evaluated analytically from Eqn 3 and was fit to the temperature-dependent slope to determine the solvent reorganization energy at each temperature (vide infra). Figure 5 shows the temperature dependent solvent reorganization energies obtained from this analysis, and Table 1 presents values for the reorganization energies at 295 K. A comparison of the 295 K reorganization energies with those predicted by the continuum model and the molecular model can be made from Table 1. In the nondipolar solvents the molecular model and the experimentally derived reorganization energies are in good agreement, whereas the continuum model predicts a reorganization energy that is much too small. The latter result is expected since the continuum model does not account for solvent quadrupoles, which are significant contributors to solvation, in these solvents. In the polar solvents, the predictions of both models deviate strongly from the experimentally derived values. Among the chlorinated solvents, the continuum model predicts that the reorganization energies in chlorobenzene, *m*-dichlorobenzene, and *m*-chlorotoluene (the three solvents with >2 D dipole moments) are comparable and are 3-fold larger than the reorganization energy in 2,5-dichlorotoluene ( $\mu = 0.57$  D). The molecular model predictions of  $\lambda_o$  are two to 3-fold larger than the continuum



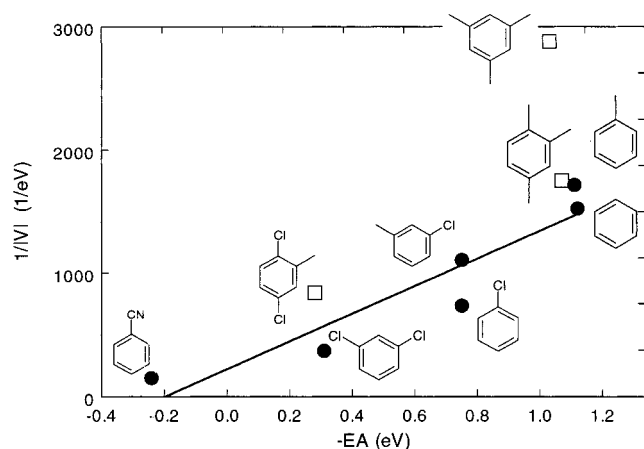
**Figure 5.** The temperature-dependent reorganization energies, predicted by the molecular-based model, are presented here for each of the solvents. The symbol convention is the same as that in Figure 4.

predictions. The molecular model also predicts that  $\lambda_o$  values among the first three solvents (chlorobenzene, *m*-dichlorobenzene and *m*-chlorotoluene) are comparable and are roughly 2-fold larger than those for 2,5-dichlorotoluene. The experimentally derived values of  $\lambda_o$  are roughly 66% larger than the values obtained from the molecular model and show similar grouping by solvent, albeit with considerably more scatter. The temperature dependence of the experimental reorganization energies are weak, Figure 5, a finding that is consistent with the weak dependence predicted by the molecular model.<sup>25</sup>

Figure 4 presents the rate constant data for the five solvents in Chart 2 and also previously published data in benzene, toluene, mesitylene, and benzonitrile. The solid curves correspond to a best fit to these data by the semiclassical expression, eq 3, using the reaction free energies (vide supra) and the internal reorganization energies found previously for 1.<sup>10</sup> The data were fit in a two step process that decoupled the electronic coupling parameter  $|V|$ , assumed to be temperature independent, from the temperature-dependent reorganization energy  $\lambda_o(T)$ . In the first step, the temperature-dependent slope was fit to obtain the reorganization energy, as described above. In the second step, the temperature-dependent reorganization energies were input to eq 3 and the  $|V|$  parameter was adjusted to fit the data. The best fit curves are displayed in Figure 4. The best fit  $|V|$  values are reported in Table 3.

The rate constants in Figure 4 are reproduced accurately by the semiclassical expression for all the solvents except mesitylene. In the latter case the rate constant displays an anomalous decline at higher temperatures. This feature of the kinetics will





**Figure 6.** The inverse of the electronic coupling is plotted as a function of  $-EA$  for different solvents. EA values are taken from ref 27. The line represents a best fit to the monosubstituted and di-substituted benzene data (filled circles). The open squares are the trisubstituted benzene data.

be discussed elsewhere.<sup>22</sup> The rate constants in the alkylbenzene solvents appear to lie near the peak of the Marcus curve (see  $\lambda_0$  in Table 1 and  $\Delta_r G$  in Figure 3), whereas the rate constant in the more polar solvents clearly lie in the normal region. The electronic couplings obtained from these fits are presented in Table 3 with the solvent molecules' electron affinity and ionization potential. The value for the electronic coupling of 2,5-dichlorotoluene is two times larger than that for the similarly shaped 1,2,4-trimethylbenzene, and the electronic coupling for *m*-dichlorobenzene is three times larger than that of the structurally similar *m*-chlorotoluene. These results are in qualitative agreement with the conclusions drawn from the continuum treatment; however, the magnitudes of the electronic coupling changes are larger in magnitude. The electronic couplings reported for the alkylbenzenes and benzonitrile are smaller than the values reported previously.<sup>6</sup> This difference arises from the different reorganization energy values used in the different analyses and reflects the sensitivity of the electronic coupling magnitude to quantitative details of the modeling.

A comparison of the electronic coupling values to the reported ionization potentials of the solvent molecules indicates no apparent correlation or dependence. A comparison of the electronic coupling magnitudes with the vertical electron affinities of the solvent molecules displays a correlation: see Figure 6. Equation 2 predicts that a plot of  $1/|V|$  versus  $(E_{D^*S-A} - E_{D^*B,A})$  should be linear. The vertical electron affinity of the solvent molecule, which is hypothesized to be proportional to the difference in energy between the transition state and the mediating superexchange state,<sup>23</sup> is used as a measure of this energy gap in Figure 6. As expected from the superexchange treatment, the graph shows a general correlation between  $-EA$  and  $1/|V|$ . This correlation shows that solvents with more positive electron affinities (more readily accept an electron) have a larger  $|V|$  than solvents with more negative electron affinities (less readily accept an electron). The value of the electronic coupling is also dependent on the solvent size and this adds a degree of scatter to the plot. The plot shows that the bulkier, trisubstituted solvents (open squares) generate a smaller electronic coupling than smaller solvents (filled circles) of a comparable electron affinity. Presumably, the more highly substituted solvents are less effective at mediating electron transfer because of their reduced ability to access geometries that have good electronic wave function overlap with the donor and acceptor moieties, described by the exchange terms in eq

2. The reasonable correlation between  $-EA$  and  $1/|V|$  indicates that electron mediated superexchange involving solvent is the dominant source of coupling in this system.

The line in Figure 6 represents a linear fit to the couplings in all the solvents that are not triply substituted; i.e., filled circles. The slope of this line ( $1123 \text{ eV}^{-2}$ ) can be used to estimate the geometric mean of the two exchange couplings  $H_{D^*S}$  and  $H_{AS}$ ;  $\beta \equiv \sqrt{H_{D^*S}H_{AS}} = 0.030 \text{ eV}$  or  $240 \text{ cm}^{-1}$ . This value is 3–6 times smaller than couplings found for cyanoanthracene–alkylbenzene contact ion pairs formed by excitation of charge-transfer complexes.<sup>24</sup> Coulomb attraction between the ions presumably reduces the separation and enhances the exchange coupling in the contact ion pairs. The estimate of  $\beta$  for **1** with aromatic solvents is only about fifteen percent larger than the  $\beta$  found for solvents spanning the wider,  $10 \text{ \AA}$  cleft of a related C-shaped molecule.<sup>8a</sup> The smaller cleft for **1** would be expected to support more extensive, simultaneous interactions between the donor, “cleft resident” solvent, and the acceptor and, therefore, to produce an even larger mean value of  $\beta$ . A difference of the electronic symmetry in the active orbitals on the donor and acceptor may act to reduce the effective mean  $\beta$  for **1**, as compared to the previously studied case.<sup>26</sup>

## Summary and Conclusions

A molecular model that describes the reaction free energy and solvent reorganization energy in alkylbenzene solvents was extended to electron-transfer studies in chlorinated benzene solvents. The previous calibration of this model for solute molecule **1** resulted in reaction free energies in the chlorinated solvents that were more negative than observed experimentally. The model was parametrized to characterize the reaction free energy at 295 K for the alkylbenzenes and dichlorotoluene. In particular, the cavity radius of the solute was increased in order to not overestimate the amount of solvation in dichlorotoluene. This procedure predicted a temperature dependence for the reaction free energy that was weaker than that observed experimentally. For the nonpolar and weakly polar solvents the temperature dependent reaction free energy was determined empirically. Although the molecular model successfully replicates the solvation provided by a homologous series of solvents; e.g., the alkylbenzenes, it fails to extrapolate well to a broader range of solvents.

To obtain an accurate modeling for the reaction free energy through the range of solvents studied here, the molecular model was fit to the experimental data in nonpolar solvents at 295 K. The reaction free energies that this model predicts in the more polar solvents are in good agreement with the values predicted by the dielectric continuum model. The temperature dependence of the reaction free energy in the polar solvents was treated as linear. Three different values of the slope ( $d\Delta_r G/dT$ ) were used in order to span a reasonable range of values. With the reaction free energy in hand, the temperature-dependent rate data was used to obtain the solvent reorganization energy and the electronic coupling magnitude. The analysis generated solvent reorganization energies that were larger than those predicted by the molecular model and the dielectric continuum model. The electronic couplings found for the aromatic solvents correlated with the vertical electron affinities of the solvent molecules; *more positive* electron affinities produce a *larger* electronic coupling for **1** than solvents with less positive electron affinities. This observation is consistent with a superexchange mechanism that predicts an increase in the electronic coupling when the energy separation between the electron-transfer transition state ( $D^*SA$ ) and the superexchange state ( $D^+S^-A$ )



is reduced. This energy separation should be smaller in solvents with more positive electron affinities. The poor correlation of  $1/|V|$  with solvent ionization potential indicates that the electronic coupling is dominated by electron mediated pathways rather than hole-mediated pathways. These data also show that more highly substituted aromatic solvents are less effective at mediating electron transfer in **1** than sparsely substituted solvents of similar electron affinity. This decreased efficiency is rationalized as an inability of the solvent to enter the cleft, and/or its decreased ability to access favorable orientations once inside the cleft.

**Supporting Information Available:** The raw rate data is provided in tabular form for the systems discussed. This material is available free of charge via the Internet at <http://pubs.acs.org>.

**Acknowledgment.** This work was supported in part by the National Science Foundation (Grants CHE-9708351 (M.B.Z.) and CHE-0111435 (D.H.W.)).

## References and Notes

- (1) (a) Jortner, J.; Bixon, M., Eds. *Electron Transfer—From Isolated Molecules to Biomolecules*. In *Advances in Chemical Physics*; Wiley: New York, 1999. (b) Barbara, P. F.; Meyer, T. J.; Ratner, M. A. *J. Phys. Chem.* **1996**, *100*, 13148.
- (2) Read, I.; Napper, A.; Zimmt, M. B.; Waldeck, D. H. *J. Phys. Chem. A* **2000**, *104*, 9385.
- (3) (a) Newton, M. D. *Chem. Rev.* **1991**, *91*, 767; (b) Jordan, K. D.; Paddon-Row, M. N. *Chem. Rev.* **1992**, *92*, 395.
- (4) (a) Nitzan, A. *J. Phys. Chem. A* **2001**, ASAP. (b) Segal, D.; Nitzan, A.; Ratner, M.; Davis, W. B. *J. Phys. Chem. B* **2000**, *104*, 2790; (c) Nitzan, A.; Jortner, J.; Wilkie, J.; Burin, A. L.; Ratner, M. A. *J. Phys. Chem. B* **2000**, *104*, 5661.
- (5) The word "rigid" is used to indicate that the bridge has only one (not multiple) minimum energy conformation.
- (6) (a) Read, I.; Napper, A.; Kaplan, R.; Zimmt, M. B.; Waldeck, D. H. *J. Am. Chem. Soc.* **1999**, *121*, 10976; (b) Kumar, K.; Lin, Z.; Waldeck, D. H.; Zimmt, M. B. *J. Am. Chem. Soc.* **1996**, *118*, 243.
- (7) (a) McConnell, H. M. *J. Chem. Phys.* **1961**, *35*, 508. (b) Newton, M. D. *Chem. Rev.* **1991**, *91*, 767. (c) Ratner, M. A. *J. Phys. Chem.* **1990**, *94*, 4877.
- (8) (a) Kaplan, R.; Napper, A. M.; Waldeck, D. H.; Zimmt, M. B. *J. Phys. Chem. A* **2002**, *106*, 1917. (b) Kaplan, R. W.; Napper, A. M.; Waldeck, D. H.; Zimmt, M. B. *J. Am. Chem. Soc.* **2000**, *122*, 12039.
- (9) If the FCWDS for each solvent pair is constant, then an increase in rate constant for the solvent pair may be linked to an enhanced electronic coupling, since
 
$$\frac{k_1}{k_2} = \frac{2\pi}{\hbar} |V_1|^2 \text{FCWDS}_1 = \frac{|V_1|^2}{|V_2|^2}$$
- (10) Kumar, K.; Kurnikov, I. V.; Beratan, D. N.; Waldeck, D. H.; Zimmt, M. B. *J. Phys. Chem. A* **1998**, *102*, 5529.
- (11) (a) Marcus, R. A. *J. Phys. Chem.* **1989**, *93*, 3078. (b) Zeng, Y.; Zimmt, M. B. *J. Phys. Chem.* **1992**, *96*, 8395.
- (12) (a) Brunschwig, B. S.; Ehrenson, S.; Sutin, N. *J. Phys. Chem.* **1986**, *90*, 3657. (b) Barzykin, A. V.; Tachiya, M. *Chem. Phys. Lett.* **1998**, *285*, 150.
- (13) (a) Jeon, J.; Kim, H. J. *J. Phys. Chem. A* **2000**, *104*, 9812. (b) Zhou, Y.; Griedman, H.; Stell, G. *J. Chem. Phys.* **1989**, *91*, 4885.
- (14) Matyushov, D. V.; Voth, G. A. *J. Chem. Phys.* **1999**, *111*, 3630.
- (15) The fluorescence decay of **1** in 1,2,4-trimethylbenzene is fit to the biexponential form:  $I(t) = a_+ e^{-k_+ t} + (1 - a_+) e^{-k_- t}$ . The forward electron-transfer rate constant  $k_{\text{for}}$  is obtained from  $k_{\text{for}} = a_+(k_+ - k_-) - k_f + k_-$ , and the reverse electron-transfer rate constant  $k_{\text{back}}$  is obtained from  $k_{\text{back}} = [(k_+ - k_-)^2 - (2k_f + 2k_{\text{for}} - k_+ - k_-)^2] / 4k_{\text{for}}$ .  $k_f$ , the donor only decay rate constant, is equated to the rate constant measured for the donor only analogue in the same solvent and temperature.
- (16) Details concerning the preparation of the DBA compound have been reported elsewhere. (a) Kumar, K.; Tepper, R. J.; Zeng, Y.; Zimmt, M. B. *J. Org. Chem.* **1995**, *60*, 4051. (b) Kaplan, R. Ph. D. Thesis, Brown University, Providence, RI, 2001.
- (17) (a) Zeglinski, D. M.; Waldeck, D. H. *J. Phys. Chem.* **1988**, *92*, 692. (b) O'Connor, D. V.; Phillips, D. *Time Correlated Single Photon Counting*; Academic Press: New York, 1984.
- (18) Kaplan, R. W.; Napper, A.; Zimmt, M. B.; Waldeck, D. H. *J. Am. Chem. Soc.* **2000**, *122*, 12039.
- (19) The parameters in the continuum calculation (cavity radius, vacuum free energy difference and dipole moment change) were chosen to match the parameters in the molecular treatment. This choice allowed a direct comparison between the two models.
- (20) The slopes found via the continuum model were 0.30 meV/K for 1,3-dichlorobenzene, 0.40 meV/K for chlorobenzene, 0.40 meV/K for chlorotoluene, and 0.12 meV/K for benzonitrile. Previous work (Vath, P.; Zimmt, M. B. *J. Phys. Chem. A* **2000**, *104*, 2626) showed that the continuum model underestimates the temperature dependence of the reaction free energy.
- (21) (a) With a temperature dependence of 2 meV/K for  $\Delta_r G$ , one finds  $\lambda_0 = 0.44$  eV and  $|V| = 9.6$  cm<sup>-1</sup> in chlorobenzene,  $\lambda_0 = 0.53$  eV and  $|V| = 16.6$  cm<sup>-1</sup> in dichlorobenzene,  $\lambda_0 = 0.37$  eV and  $|V| = 6.9$  cm<sup>-1</sup> in *meta*-chlorotoluene, and  $\lambda_0 = 1.0$  eV and  $|V| = 42$  cm<sup>-1</sup> in benzonitrile. (b) With the continuum model's temperature dependence for  $\Delta_r G$  (see ref 20), one finds  $\lambda_0 = 0.51$  eV and  $|V| = 12$  cm<sup>-1</sup> in chlorobenzene,  $\lambda_0 = 0.68$  eV and  $|V| = 31$  cm<sup>-1</sup> in dichlorobenzene,  $\lambda_0 = 0.42$  eV, and  $|V| = 8.1$  cm<sup>-1</sup> in *meta*-chlorotoluene, and  $\lambda_0 = 1.1$  eV and  $|V| = 65$  cm<sup>-1</sup> in benzonitrile.
- (22) Napper, A.; Waldeck, D. H.; Zimmt, M. B. *J. Phys. Chem.* In press.
- (23) For the situation in which the solvent mediated pathway dominates the other contributions to the electronic coupling magnitude, the superexchange state is depicted by D<sup>+</sup>S<sup>-</sup>A (for a reaction "mechanism" of D<sup>\*</sup>SA → D<sup>+</sup>S<sup>-</sup>A → D<sup>+</sup>SA<sup>-</sup>). Between the different solvent systems being studied, the major change in energetics of the superexchange state will arise from the energetics of S<sup>-</sup>. The solvent dependence of the donor's ionization potential is assumed to be small. Hence, the electron affinity of the solvent gauges the change in energetics.
- (24) Gould, I. R.; Young, R. H.; Mueller, L. J.; Albrecht, A. C.; Farid, S. *J. Am. Chem. Soc.* **1994**, *116*, 8188.
- (25) The apparent, slight increase of the solvent reorganization energy with temperature (Figure 5) does not agree with the slight decrease observed in experiments<sup>20</sup> or predicted by modern solvation theory.<sup>14</sup> This slight difference is likely a result of the assumed temperature independence of the electronic coupling. See ref 22.
- (26) Cave, R. J.; Newton, M. D.; Kumar, K.; Zimmt, M. B. *J. Phys. Chem.* **1995**, *99*, 17501.
- (27) (a) Jordan, K. D.; Michejda, J. A.; Burrow, P. D. *J. Am. Chem. Soc.* **1976**, *98*, 7189. (b) Burrow, P. D.; Modeli, A.; Jordan, K. D. *Chem. Phys. Lett.* **1986**, *132*, 441. (c) Burrow, P. D.; Howard, A. E.; Johnston, A. R.; Jordan, K. D. *J. Phys. Chem.* **1992**, *96*, 7570 and references therein.
- (28) (a) Matyushov, D. V.; Schmid, R. *J. Chem. Phys.* **1996**, *104*, 8627. (b) Ben-Amotz, D.; Willis, K. G. *J. Phys. Chem.* **1993**, *97*, 7736.